Catalysis Today 158 (2010) 241–245

Contents lists available at ScienceDirect

Catalysis Today

journal homepage: www.elsevier.com/locate/cattod

Iron carbide promoted K/β-Mo_2C for higher alcohols synthesis

Ning Wang[a,b], Kegong Fang[a], Dong Jiang[a], Debao Li[a], Yuhan Sun[a,*]

[a] State Key Laboratory of Coal Conversion, Shanxi Institution of Coal Chemistry, Chinese Academy of Sciences, 27#, Taoyuan South Road, Taiyuan, Shanxi 030001, PR China
[b] Graduate University of the Chinese Academy of Sciences, Beijing 100039, PR China

ARTICLE INFO

Article history:
Available online 3 June 2010

Keywords:
Iron carbide modified
K/β-Mo_2C
Higher alcohols synthesis
Syngas

ABSTRACT

Iron carbide promoted K/β-Mo_2C catalysts were prepared and tested for higher alcohols synthesis. The results revealed that β-Mo_2C produced mainly hydrocarbons, but the addition of potassium resulted in a remarkable selectivity shift from hydrocarbons to alcohols and then a higher selectivity to C_2^+OH over β-Mo_2C. Moreover, it was found that iron carbide further enhanced the selectivity of higher alcohols, showing the optimum at 1/6 of Fe/Mo molar ratio. The corresponding characterization suggested that there might be a synergistic effect of iron carbide and K/β-Mo_2C, i.e. the formation of "K-Fe-Mo-C" species which favored the alcohols synthesis.

1. Introduction

The development of highly active and selective catalysts for the production of higher alcohols becomes increasingly important as the application in the fuel and chemical industries [1]. As a new type of catalyst, molybdenum carbide has been reported to be active for the synthesis of light hydrocarbons in the liquefied petroleum gas range from syngas [2,3]. Woo et al. [4] found that the promotion of molybdenum carbide with K_2CO_3 could greatly enhance the selectivity for linear C_1–C_7 alcohols. In our previous work [5], the effects of Fischer–Tropsch (F–T) elements (Fe, Co and Ni) were used as promoters for higher alcohols synthesis via syngas over K/β-Mo_2C catalyst. Such F–T elements modified K/β-Mo_2C catalysts appeared to be highly active and selective towards the synthesis of mixed alcohols, but their performance is not satisfactory enough for the practical application.

From the literatures reviewed, the physical phase of the iron carbides played an important role in F–T synthesis [6–8]. Amelse et al. reported that iron carbides on the catalysts surface to be the active phase [9]. Ando et al. revealed that iron carbide was the active site for hydrocarbon formation, and the site for C_2^+OH formation was relevant to the hydrocarbon formation site [10]. However, iron carbide was seldom investigated and rarely reported as a promoter to Mo_2C catalyst. Thus, a series of iron carbide promoted K/β-Mo_2C catalyst was investigated for the higher alcohols synthesis in the present work.

2. Experimental

2.1. Catalyst preparation

The samples of molybdenum carbide and iron carbide were prepared by the temperature-programmed-reaction (TPRe) method. In detail, the β-Mo_2C and iron carbide were prepared by direct carburization of the MoO_3 and Fe_2O_3 precursors, respectively. For β-Mo_2C, TPRe was carried out under atmospheric pressure in a flow of CH_4/H_2 (1/4, V/V) gas mixture. The gas hourly space velocity was of 6000 h^{-1}. The temperature was linearly increased at the rate of 1 °C/min from room temperature to 700 °C, where it was maintained for 4 h. Then the samples were quenched to room temperature in a flow of argon and gradually passivated with 1 v% O_2/Ar until complete saturation of the surface. For the iron carbide, TPRe was carried out under atmospheric pressure in a flow of pure CO gas. The gas hourly space velocity was of 6000 h^{-1}. The temperature was linearly increased at the rate of 1 °C/min from room temperature to 400 °C, where it was maintained for 4 h. Then the samples were quenched to room temperature in a flow of argon and gradually passivated with 1 v% O_2/Ar until complete saturation of the surface. Then the β-Mo_2C, iron carbide and K_2CO_3 were physically mixed in a mortar with the required molar ratio. The iron carbide promoted K/β-Mo_2C (denoted as Fe/K/β-Mo_2C) catalyst was finally obtained by calcining the mixture at 773 K for 4 h.

2.2. Catalyst characterization

BET surface areas of catalysts were determined by N_2 adsorption at −196 °C using ASAP-2000 Micromeritics instrument. X-ray power diffraction (XRD) patterns of the catalysts were conducted on PANalytical X'pert pro diffractometer using Cu Kα radiation.

---

* Corresponding author. Tel.: +86 351 4121877.
E-mail address: yhsun@sxicc.ac.cn (Y. Sun).

0920-5861/$ – see front matter © 2010 Elsevier B.V. All rights reserved.
doi:10.1016/j.cattod.2010.03.079

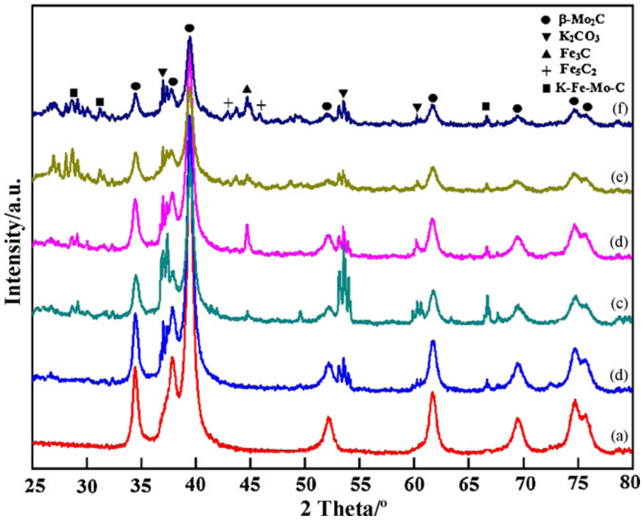

Fig. 1. XRD patterns of the samples (a) β-Mo_2C, (b) K/β-Mo_2C, (c) Fe/Mo = 1:8, (d) Fe/Mo = 1:6, (e) Fe/Mo = 1:4 and (f) Fe/Mo = 1:2.

The crystallite size was calculated by X'Pert HighScore Plus software. Scanning electron microscopy (SEM) images were carried out using a Hitachi S-4800 microscope. The X-ray Photoelectron Spectra (XPS) were recorded on a XSAM800 spectrometer (Kratos, U.K.) using an Al Kα X-ray source, the base pressure of the chamber was less than 2×10^{-7} Pa. The binding energy was corrected with the energy of C1s (284.8 eV) for carbon contaminant.

2.3. *Catalyst test*

The catalytic reactions were carried out using a stainless steel fixed-bed reactor with 1.0 mL (40–60 mesh) of catalyst. The reaction conditions were as follows: $T = 613$ K, $P = 7.0$ Mpa, GHSV = 4000 h^{-1}, $n(H_2)/n(CO) = 2.0$. Both gaseous and liquid products were analyzed off-line by gas chromatographs. H_2, CO, CH_4 and CO_2 were determined by thermal conductivity detector (TCD) with a TDX-101 column. The water and methanol in liquids were also detected by TCD with a GDX-401 column. The alcohols were analyzed by flame ionization detector (FID) with a Porapack-Q column. The carbon balance and mass balance were 100 ± 5%.

3. Results and discussion

3.1. *Phase and texture*

The XRD patterns of the samples are shown in Fig. 1, and β-Mo_2C-based catalysts all had a definitive phase of molybdenum carbide with hexagonal close packed (HCP) structure [11], respectively). With the promotion by potassium, the intensity of peaks assigned to β-Mo_2C became slightly weak. Meanwhile, the new diffraction peaks appeared at 2θ values of 31.6°, 32.2°, 37.5° and 49.1° due to the formation of K_2CO_3 [12], and the larger β-Mo_2C particles were produced with the addition of K_2CO_3. Besides β-Mo_2C and K_2CO_3 phase [11,12], new peaks appeared at 42.8°, 43.7°, 44.3°, 43.9°, 44.6° and 45.8° for Fe carbide promoted K/β-Mo_2C, which could be attributed to Fe_3C (JCPDS 350772) and Fe_5C_2 (JCPDS 200508) phase, respectively. The XRD data of β-Mo_2C in all samples indicated that the crystallite size of β-Mo_2C increased by both K and iron carbide (see Table 1). In addition, new diffraction peaks were observed at 28.8, 31.1, 49.5 and 66.7, which were closely related to the complex compound of K, Fe and β-Mo_2C, i.e. "K–Fe–Mo–C" entities [5].

Table 1
Physical Characteristics of samples.

Catalyst	Crystallite size (nm)	BET surface area (m^2/g)	Pore volume (cm^3/g)
β-Mo_2C	13.1	10.29	9.8×10^{-3}
K/β-Mo_2C	14.6	6.52	7.1×10^{-3}
Fe/Mo = 1/8	15.3	5.46	6.5×10^{-3}
Fe/Mo = 1:6	16.1	4.37	5.8×10^{-3}
Fe/Mo = 1:4	19.2	4.21	5.3×10^{-3}
Fe/Mo = 1/2	21.1	3.95	4.9×10^{-3}

SEM micrographs indicated that β-Mo_2C showed the regular morphology of hexagonal particles (see Fig. 2). However, the addition of potassium led to the formation of small clusters on the surface of β-Mo_2C, which were due to the presence of K_2CO_3 and/or "K-Mo-C" particles as reported in the previous work [13]. Such different change was more evident for Fe carbide promoted K/β-Mo_2C catalyst (see Fig. 2c). Combined with XRD, it seemed that iron carbide almost inserted into the bulk β-Mo_2C and existed in the form of "K–Fe–Mo–C" particles. As the catalysts for mixed alcohols synthesis, such an interaction between Mo and promoters would have a great influence on the catalytic performance [14,15].

All the samples showed a low BET surface areas less than 11 m^2/g along with low pore volume ($<1.0 \times 10^{-2}$ cm^3/g). This indicated that they were almost nonporous.

3.2. *Surface properties*

The Mo3d XPS spectra are presented in Fig. 3. The binding energy (B.E.) at 229.4 and 228.2 eV could be attributed to the Mo $3d_{5/2}$, corresponding to Mo^{4+} and Mo^{2+} species, respectively [11]. The carbide phase was involved in Mo $3d_{5/2}$ peak at low B.E. (228.2 eV) [17]. Being promoted by potassium, the binding energy shifted to a lower value, and a new peak appeared around 227.5 eV due to the presence of Mo^0 or Mo^δ ($0 < \delta < 2$) [11]. Doped by iron carbide and potassium, however, the chemical environment of Mo displayed an obvious diversification. Besides the increase in Mo^{4+} and Mo^{2+} along with the appearance of Mo^0, the lower B.E. of Mo $3d_{5/2}$ than K/β-Mo_2C could be due to the strong interaction between Fe and Mo species. According to the results of XRD and SEM, the interaction might be attributed to the formation of "K–Fe–Mo–C" species.

The XPS spectra of Fe 2p had two large peaks at 724.6 and 711.6 eV for the Fe $2p_{1/2}$ and Fe $2p_{3/2}$ transitions, respectively [18]. Simultaneously, a narrow Fe $2p_{3/2}$ peak appearing at 706.9 eV was characteristic of iron in iron carbides [19], which was considered to increase the selectivity towards oxygenates [20]. In addition, A weak shoulder peak appeared at 715.6 eV due to the presence of reduced Fe^{2+} [19].

The surface composition of β-Mo_2C-based catalysts is listed in Table 2. The enrichment of K and Fe indicated that they existed in the form of "K-Mo-C" or K–Fe–Mo–C" on the surface of K/β-Mo_2C and Fe carbide promoted K/β-Mo_2C catalysts, respectively. Moreover, the higher ratio of carbon to molybdenum suggested

Table 2
Surface composition of the catalysts (calculated from XPS data).

Catalyst $n(Fe)/n(Mo)$	Surface composition/mol%				
	Mo	Fe	K	C	O
β-Mo_2C	12.68	–	–	57.41	28.75
K/β-Mo_2C	11.76	–	6.43	52.78	29.03
1/8	4.76	1.44	4.63	72.13	17.05
1/6	5.53	1.68	4.86	67.48	20.45
1/4	5.64	2.51	4.97	61.87	24.53
1/2	6.12	3.64	5.12	63.20	22.40
1/6[a]	5.38	1.76	4.93	65.37	22.56

[a] Surface composition after ending the induction period.

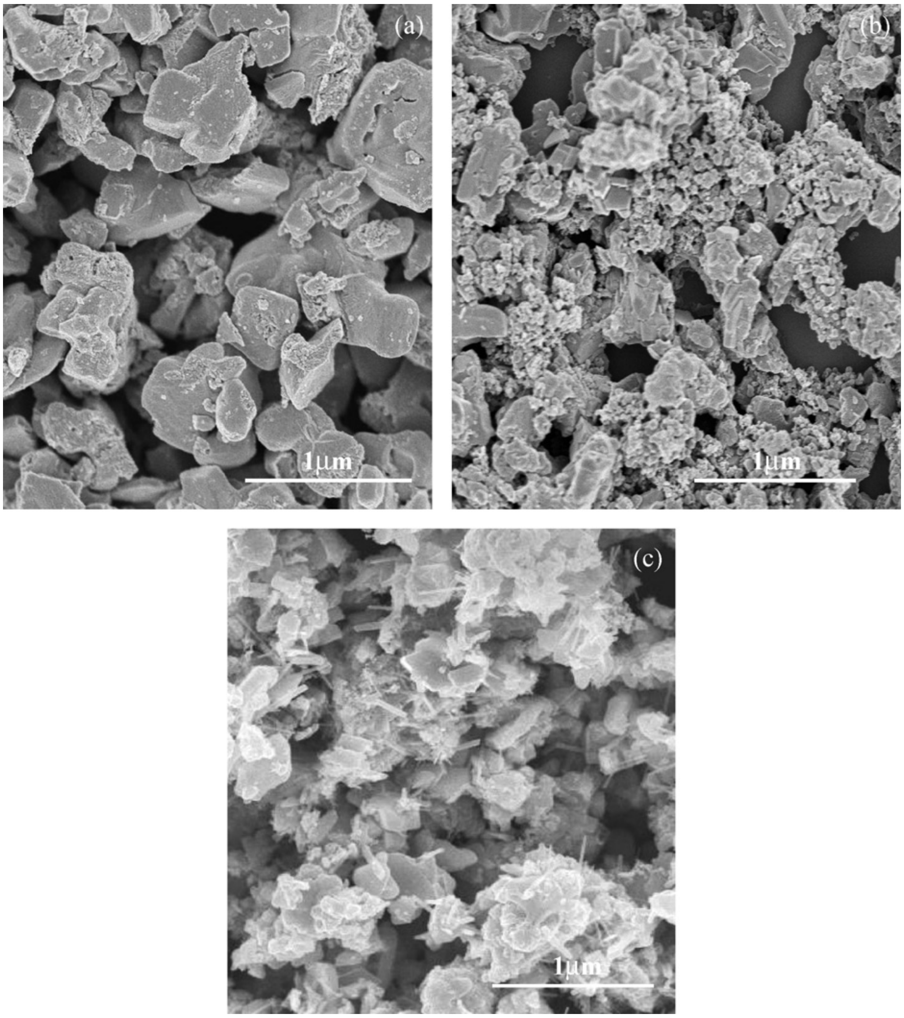

Fig. 2. Typical SEM image of samples (a) β-Mo_2C, (b) K/β-Mo_2C and (c) Fe/K/β-Mo_2C.

that amorphous carbon might be deposited on the catalysts [21].

3.3. Catalytic performance

As shown in Table 3, CO hydrogenation overβ-Mo_2C catalyst mainly produced hydrocarbons, and with modified by potassium, the products shifted to both hydrocarbons and alcohols with the yield of alcohols of 0.12 g/ml h. The addition of iron carbide into K/β-Mo_2C catalyst led to a sharp increase in both activity and selectivity to $C_2{}^+OH$ products, and the proportion of methanol was greatly suppressed and $C_2{}^+OH$ alcohols became the major liquid products. This indicated that iron carbide had a strong ability to promote the chain growth. The optimal molar ratio of Fe/Mo was about

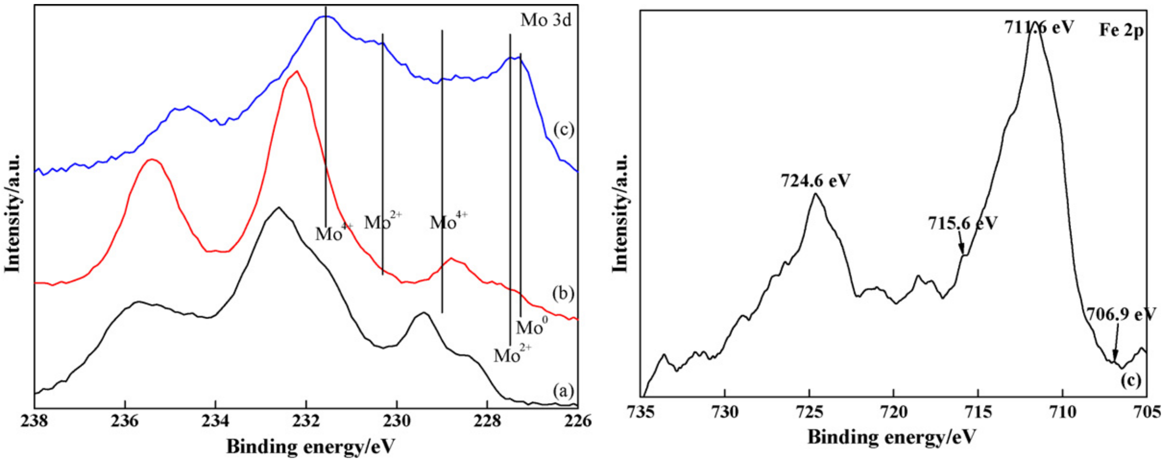

Fig. 3. Mo 3d XPS and Fe 2p spectra of samples (a) β-Mo_2C, (b) K/β-Mo_2C and (c) Fe/K/β-Mo_2C.

Table 3
Performance of CO hydrogenation over catalysts.

Catalyst	CO Conv. (%)	Selectivity[a] (wt%)		ROH distribution (wt%)		Yield (g/(ml h))	
		ROH	HC	MeOH	C_2^+OH	ROH	C_2^+OH
β-Mo_2C	75.89	5.24	94.76	83.88	16.12	0.02	–
K-β-Mo_2C	50.96	34.66	65.34	38.86	61.14	0.12	0.04
Fe/Mo[b] = 1/8	55.18	37.81	62.19	34.00	66.00	0.13	0.05
Fe/Mo[b] = 1/6	86.92	41.47	58.53	20.96	79.04	0.23	0.14
Fe/Mo[b] = 1/4	80.31	36.56	63.44	26.64	73.36	0.19	0.10
Fe/Mo[b] = 1/2	70.84	35.65	64.35	26.66	73.34	0.14	0.06

Reaction conditions: $T = 613$ K, $P = 7.0$ Mpa, GHSV = 4000 h^{-1}, $n(H_2)/n(CO) = 2.0$.

[a] Free of CO_2.

[b] Fe/Mo for the molar ratio of iron and molybdenum in catalysts.

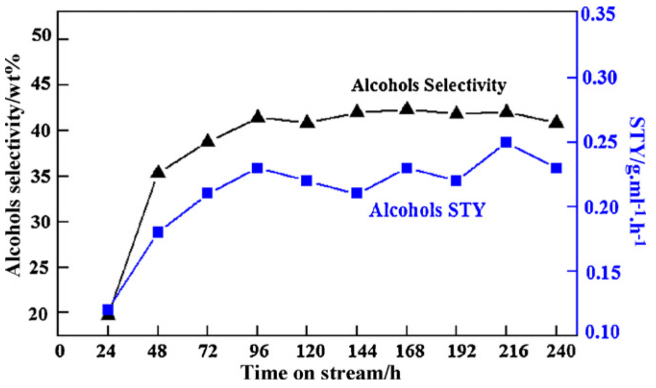

Fig. 4. Stability test of Fe/K/β-Mo_2C catalyst with Fe/Mo = 1:6.

1/6 for Fe carbide promoted K/β-Mo_2C catalyst, at which a high CO conversion reached 86.92% with the maximum alcohol yield of 0.23 g/ml h. In terms of catalytic performance, the increase in the number of Mo^{4+} on the surface of β-Mo_2C might favor the alcohols synthesis, whereas the lower valence of Mo ($Mo^{2+}$and Mo^0) might favor the hydrocarbons synthesis [22,23]. In the present case, both high activity and selectivity for alcohols might be closely related to the "K–Fe–Mo–C" structure which were analogous to "K–Co–Mo–S" in the K/Co/MoS_2 catalyst [24].

Fig. 4 shows the changes in space-time-yield (STY) and selectivity of alcohols with time on stream. For Fe carbide promoted K/β-Mo_2C catalyst with Fe/Mo = 1/6, it could be found that there existed an induction period at the initial stage. With the time on stream, the STY and selectivity increased gradually and reached a steady state after 96 h. The similar trend was observed for other Fe carbide promoted K/β-Mo_2C catalysts with different Fe/Mo ratios.

For molybdenum carbide, deposited carbon species might be eliminated during the induction period [3], and it was also reported that during the induction period, a part of the surface oxygen on the β-Mo_2C-based catalyst probably reacted with carbon and was removed from the uppermost surface layer during the induction period [25].

3.4. Roles of potassium and iron in the chain growth

Fig. 5 gives the distribution of alcohols and hydrocarbons described by the Anderson–Schulz–Flory (A–S–F) equation: $M_n = P^{n-1}(1 - \mathrm{P})$, where M_n is the mole fraction of the product with a carbon number of n and P is the chain-growth probability [26,27]. For β-Mo_2C catalyst, the chain-growth probability of P for alcohols and hydrocarbons were 0.11 and 0.25, respectively, and their distribution showed the similar linear A–S–F plots. With the addition of potassium, hydrocarbons and C_2–C_4 alcohols still displayed the linear A–S–F plot but methanol showed a deviation. This indicated a different reaction mechanism for the formation of alcohols over K-β-Mo_2C catalyst. Compared with the chain-growth probability P for alcohols and hydrocarbons, potassium played the role in the improvement of the probability. With both potassium and iron carbide as promoters, the A–S–F plots of hydrocarbons showed the similar types to Mo_2C and alcohols to K-β-Mo_2C catalyst, and the chain-growth probability of alcohols and hydrocarbons had the similar trends (see Fig. 5). Thus, both potassium and iron carbide had a positive effect on the chain growth.

Generally, Fe carbide in the promoted β-Mo_2C catalyst has a dual function in CO hydrogenation. It favored the higher alcohols synthesis due to its strong ability of CO insertion, and also promoted the hydrocarbons synthesis due to its strong ability of CO

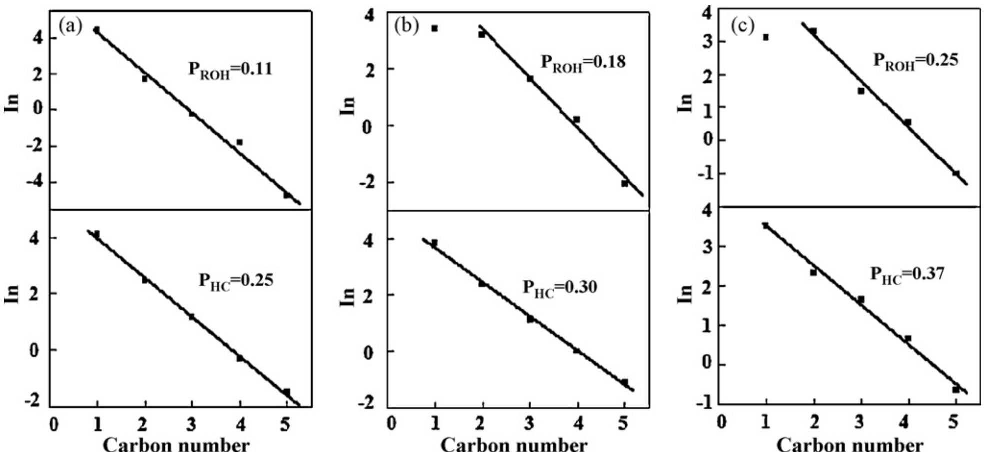

Fig. 5. A–S–F plots of alcohols and hydrocarbons over the different catalysts (a)β-Mo_2C (b) K-β-Mo_2C (c) Fe/K/β-Mo_2C.

dissociation [5,28]. According to the literature [29], iron carbide showed the superior activity in hydrogenation. Compared with our previous work [5], iron carbide promoted catalyst showed the better catalytic performance at a relatively lower pressure and a high molar ratio of H_2/CO.

As for the formation of higher alcohols, it was most important to understand how the first chain-growth step (C_1–C_2) took place, and then with C_1 species involved, the other was to account for the deviation from the A–S–F distribution for the preferment formation of higher alcohols [15,16]. The main difference between Fe carbide promoted K/β-Mo_2C and β-Mo_2C catalysts resulted from the chain propagation of C_1OH to C_2OH. For β-Mo_2C catalyst, the formation of hydrocarbons corresponded to a polymerisation of CH_x species as the products obeyed the Schulz–Flory rule. For iron carbide promoted K/β-Mo_2C catalyst, a surface phase such as “K–Fe–Mo–C” might be responsible for the production of $C_2{}^+OH$, especially for the C_1 to C_2 conversion. In general, the linear chain growth via C_1 intermediate insertion at the end of chain resulted in linear primary alcohols. In the present case, the formation of linear primary alcohols would take place via CO insertion. Besides, iron carbide showed superior activity in hydrogenation [29]. Due to the function of potassium and iron carbide, analogous as K–Co–Mo–S, it was likely that the “K–Fe–Mo–C” phase was the active site for the alcohols synthesis over iron carbide promoted K/β-Mo_2C catalyst.

4. Conclusions

Both alcohols and hydrocarbons were produced for iron carbide promoted β-Mo_2C in the presence of potassium. Potassium led to a remarkable shift of the products from hydrocarbons to alcohols. With promoted by both potassium and iron carbide, the catalyst showed to be highly active and selective towards the formation of $C_2{}^+OH$ with the maximum at Fe/Mo molar ratio of 1/6. This was due to the strong promotion for carbon chain growth by iron carbide, especially for the stage of C_1OH to C_2OH. The “K–Fe–Mo–C” phase might be the active site for the alcohols synthesis over iron carbide promoted K/β-Mo_2C catalyst.

Acknowledgments

The authors gratefully acknowledge the financial support from National Natural Science Foundation of China for Project No. 20590363 and Shell for Higher Alcohols Synthesis Package.

References

[1] G.A. Mills, Fuel 73 (1994) 1243.
[2] P.M. Patterson, T.K. Das, B.H. Davis, Appl. Catal. A: Gen. 251 (2003) 449.
[3] A.G. Constant, J.M. Giraudon, G. Leclercq, L. Leclercq, Appl. Catal. A 260 (2004) 35.
[4] H.C. Woo, K.Y. Park, Y.G. Kim, I. Nam, J.S. Chung, J.S. Lee, Appl. Catal. 75 (1991) 267.
[5] M.L. Xiang, D.B. Li, H.C. Xiao, J.L. Zhang, H.J. Qi, W.H. Li, B. Zhong, Y.H. Sun, Fuel 87 (2008) 599.
[6] J.W. Niemantsverdriet, A.M. van der Kraan, W.L. van Dijk, H.S. van der Baan, J. Phys. Chem. 84 (1980) 3363.
[7] W.S. Ning, N. Koizumi, H. Chang, T. Mochizuki, T. Itoh, M. Yamada, Appl. Catal. A 312 (2006) 35.
[8] J.B. Butt, Catal. Lett. 7 (1990) 61.
[9] J.A. Amelse, J.B. Butt, L.H. Schwartz, J. Phys. Chem. 82 (1978) 558.
[10] H. Ando, Y. Matsumura, Y. Souma, Appl. Organomet. Chem. 14 (2000) 831.
[11] K. Oshikawa, M. Nagai, S. Omi, J. Phys. Chem. B 105 (2001) 9124.
[12] J. Iranmahboob, D.O. Hill, H. Toghiani, Appl. Surf. Sci. 185 (2001) 72.
[13] M.L. Xiang, D.B. Li, H.J. Qi, W.H. Li, B. Zhong, Y.H. Sun, Fuel 86 (2007) 1298.
[14] J. Bao, Y.L. Fu, Z.H. Sun, C. Gao, Chem. Commun. 6 (2003) 746.
[15] G.Z. Bian, Y.L. Fu, Y.S. Ma, Catal. Today 51 (1999) 187.
[16] Z.R. Li, Y.L. Fu, M. Jiang, Catal. Lett. 65 (2000) 43.
[17] T.P.S. Clair, S.T. Oyama, D.F. Cox, S. Otani, Y. Ishizawa, R.-L. Lo, K.-I. Fukui, Y. Iwasawa, Surf. Sci. 426 (1999) 187.
[18] C.S. Kuivila, J.B. Butt, P.C. Stair, Appl. Surf. Sci. 32 (1988) 99.
[19] D.J. Dwyer, J.H. Hardenbergh, J. Catal. 87 (1984) 66.
[20] M.Y. Ding, Y. Yang, J. Xu, Z.C. Tao, H.L. Wang, H. Wang, H.W. Xiang, Y.W. Li, Appl. Catal. A: Gen. 345 (2008) 176.
[21] H. Zheng, D. Ma, X. Liu, W. Zhang, X. Han, Y. Xu, X.H. Bao, et al., Catal. Lett. 111 (2006) 111.
[22] A. Muramatsu, T. Tatsumi, H. Tominaga, J. Phys. Chem. 96 (1992) 1334.
[23] Y. Zhang, Y. Sun, B. Zhong, Catal. Lett. 76 (2001) 249.
[24] D.B. Li, C. Yang, W.H. Li, Y.H. Sun, B. Zhong, Top. Catal. 32 (2005) 233.
[25] W.C. Wu, Z.L. Wu, C.H. Liang, J. Phys. Chem. B 107 (2003) 7088.
[26] R.B. Anderson, Catalysts for the Fischer–Tropsch Synthesis, Van Nostrand Reinhold, New York, 1956, Vol. 4.
[27] X.G. Liu, L.J. Feng, Z.Y. Liu, B. Zhong, D.B. Dadyburjor, E.L. Kugler, Ind. Eng. Chem. Res. 37 (1998) 3853.
[28] J.S. Lee, L. Volpe, F.H. Ribeiro, M. Boudart, J. Catal. 112 (1988) 44.
[29] I.K. Milad, K.J. Smith, P.C. Wong, K.A.R. Mitchell, Catal. Lett. 52 (1998) 113.